



<sup>a</sup>Department of Biomedical Engineering, University of North Carolina, Chapel Hill, NC, USA, North Carolina State University, Raleigh, NC, USA;

<sup>b</sup>Division of Cardiothoracic Surgery and; <sup>c</sup>Division of Pulmonary Diseases and Critical Care Medicine; <sup>d</sup>Division of Pharmacoengineering and Molecular Pharmaceutics, University of North Carolina, Chapel Hill, NC, USA;

<sup>e</sup>Department of Molecular Biomedical Sciences and Comparative Medicine Institute; <sup>f</sup>Department of Biology; <sup>g</sup>Department of Molecular and Structural Biochemistry, North Carolina State University, Raleigh, NC, USA; <sup>h</sup>The Third Hospital of Hebei Medical University, Shijiazhuang, Hebei, People's Republic of China; <sup>i</sup>Children's Hospital of Hebei Province, Shijiazhuang, Hebei, People's Republic of China; <sup>j</sup>Hebei Chest Hospital, Shijiazhuang, Hebei, People's Republic of China; <sup>k</sup>First Affiliated Hospital of Zhengzhou University, Henan, People's Republic of China

Correspondence: Ke Cheng, Ph.D., 1060 William Moore Drive, Raleigh, North Carolina 27607, USA. Telephone: 919-513-6157; Fax: 919-513-7301; e-mail: ke\_cheng@ncsu.edu or ke\_cheng@unc.edu or Leonard Jason Lobo M.D., 8006 Burnett-Womack Building Chapel Hill, North Carolina 27514, USA. Telephone: 919-966-2531; Fax: 984-974-6822; e-mail: jason\_lobo@med.unc.edu

Received August 10, 2016; accepted for publication June 1, 2017; first published August 7, 2017.

<http://dx.doi.org/10.1002/sctm.16-0374>

This is an open access article under the terms of the Creative Commons Attribution-NonCommercial-NoDerivs License, which permits use and distribution in any medium, provided the original work is properly cited, the use is non-commercial and no modifications or adaptations are made.

## Safety and Efficacy of Allogeneic Lung Spheroid Cells in a Mismatched Rat Model of Pulmonary Fibrosis

JHON CORES ,<sup>a,e</sup> M. TAYLOR HENSLEY,<sup>e</sup> KATHRYN KINLAW,<sup>f</sup> S. MICHAELA RIKARD,<sup>a</sup> PHUONG-UYEN DINH,<sup>e</sup> DIPTI PAUDEL,<sup>g</sup> JUNNAN TANG,<sup>e,k</sup> ADAM C. VANDERGRIF,<sup>a,e</sup> TYLER A. ALLEN,<sup>e</sup> YAZHOU LI,<sup>h</sup> JIANHUA LIU,<sup>i</sup> BO NIU,<sup>i</sup> YUEPENG CHI,<sup>j</sup> THOMAS CARANASOS,<sup>b</sup> LEONARD J. LOBO,<sup>c</sup> KE CHENG<sup>a,d,e</sup>

**Key Words.** Fibrosis • Pulmonary • Syngeneic • Allogeneic • Stem cells

### ABSTRACT

Idiopathic pulmonary fibrosis is a devastating interstitial lung disease characterized by the relentless deposition of extracellular matrix causing lung distortions and dysfunctions. The prognosis after detection is merely 3–5 years and the only two Food and Drug Administration-approved drugs treat the symptoms, not the disease, and have numerous side effects. Stem cell therapy is a promising treatment strategy for pulmonary fibrosis. Current animal and clinical studies focus on the use of adipose or bone marrow-derived mesenchymal stem cells. We, instead, have established adult lung spheroid cells (LSCs) as an intrinsic source of therapeutic lung stem cells. In the present study, we compared the efficacy and safety of syngeneic and allogeneic LSCs in immunocompetent rats with bleomycin-induced pulmonary inflammation in an effort to mitigate fibrosis development. We found that infusion of allogeneic LSCs reduces the progression of inflammation and fibrotic manifestation and preserves epithelial and endothelial health without eliciting significant immune rejection. Our study sheds light on potential future developments of LSCs as an allogeneic cell therapy for humans with pulmonary fibrosis. *STEM CELLS TRANSLATIONAL MEDICINE* 2017;9:1905–1916

### SIGNIFICANCE STATEMENT

We have demonstrated the safety and efficacy of allogeneic lung spheroid cell (LSC) treatment in attenuating the progression and severity of pulmonary fibrosis, decreasing apoptosis, protecting alveolar structures, and increasing angiogenesis in rats. The use of allogeneic stem cells can potentially change the way we perform cell therapies by allowing for the growth of large quantities of cells from numerous sources, including donated lungs not used for transplantations, surgical discards, and lungs from recently deceased cadavers. Our study demonstrates the potential of allogeneic LSCs as a viable future therapy option for patients suffering from idiopathic pulmonary fibrosis.

### INTRODUCTION

Idiopathic pulmonary fibrosis (IPF) is a chronic, progressive, life-threatening disease, characterized by thickening, stiffening, and scarring of the lung interstitium, resulting in poor oxygen acquisition and exertional dyspnea. The prevalence of IPF in the U.S. has been estimated to be between 14 and 43 per 100,000 persons, and its rate of incidence between 7 and 16 per 100,000 persons [1]. As recently as 2014, treatment of IPF was limited to oxygen therapy, pulmonary rehabilitation, and eventual lung transplantation. As of October 2014, two Food and Drug Administration approved pharmaceuticals, Esbriet and Ofev, were added to the arsenal of tools available to combat the disease. The

drugs, however, are palliative not curative, and come with a number of side effects, including rashes, nausea, diarrhea, and lack of energy [2].

Stem cell therapy has emerged as a promising alternative to pharmacological treatments for various diseases [3–8]. Clinical and preclinical research focuses on mesenchymal stem cells (MSCs) derived from bone marrow or adipose tissue. Our group, instead, has established adult lung spheroid cells (LSCs) as an intrinsic source of therapeutic lung stem cells. In a xenogeneic transplantation model, we demonstrated the regenerative potential of human LSCs in immunodeficient mice with bleomycin-induced interstitial lung disease [9]. We have also demonstrated the superior performance of LSCs over adipose-derived MSCs in a syngeneic rat model that sought to slow the

rate of development and severity of lung fibrosis [9]. A major drawback of autologous therapy is the need for patients to wait for their cells to expand after an intrusive biopsy procedure. It is not clear, however, whether allogeneic LSC therapy will trigger immune rejection and, if so, whether side effects can be managed with an acceptable benefit/risk ratio. To that end, we sought to determine the safety and efficacy of allogeneic LSCs in attenuating the progression of pulmonary fibrosis in a rat model. To create a stringent model of allogeneic cell transplantation, we used rats from highly-inbred, immunologically-divergent strains characterized by complete mismatch of major histocompatibility complex (MHC) antigens. Male Wistar-Kyoto (WKY) rats (MHC haplotype, RT<sup>I</sup>) were used as LSC donors while female WKY and Brown Norway (BN) rats (MHC haplotype, RT<sup>II</sup>) were used as syngeneic and allogeneic recipients, respectively.

## MATERIALS AND METHODS

### LSC Culture

Healthy rat lung tissues were excised from three 6-week-old syngeneic Wistar Kyoto rats. Approximately 5–10 mm samples of distal lung tissue were separated and washed with phosphate-buffered saline (PBS) (Life Technologies, Carlsbad, CA, <http://www.lifetechnologies.com>) to remove excess blood. The tissue samples were then cut into smaller 2 mm pieces, washed three times with PBS, and enzymatically digested at 37°C in 5 mg/ml collagenase type IV solution (Sigma-Aldrich, St. Louis, MO, <http://www.sigmaaldrich.com>). Collagenase digestion was inactivated after 5 minutes using an equal volume of Iscove's modified Dulbecco's medium (IMDM; Life Technologies) containing 20% fetal bovine serum (FBS; Corning Life Sciences, Acton, MA, <http://www.corning.com/>). Subsequently, the tissue samples were minced into smaller tissue bits (0.5–1 mm) before being plated onto 150 mm fibronectin-coated petri dishes in 2 ml of 20% FBS IMDM overnight to allow tissue-plate adhesion to take place. The next day, 20 ml of media were added into the dish. The tissues were kept in media for approximately 1 week (or until cells began to outgrow from the tissue explants) during which media was changed once every other day. At a confluence of approximately 70%–80%, outgrowth cells were harvested from the petri dishes via 5–10 minutes of incubation with TryPLE Select (Life Technologies). The cells were passaged into ultra-low attachment flasks (Corning Life Sciences) at a density of 100,000 cells per cm<sup>2</sup> and cultured with 10% FBS IMDM. Within 24–36 hours, spontaneous spheroid formation was observed and allowed to mature for up to a week. Lung spheroids were then collected and replated onto fibronectin-coated flasks (Corning Life Sciences) to generate adherent LSCs. These were cultured in 20% FBS IMDM containing 50 mg/ml gentamicin (Life Technologies), 2 mmol/l L-glutamine (Life Technologies), and 0.1 mmol/L 2-mercaptoethanol (Life Technologies). The growth rate of the cells was assessed in terms of cumulative doublings per time.

### Flow Cytometry

Flow cytometry was used to determine the antigenic phenotypes of LSCs. Rat LSCs were incubated with anti CD105, CD90, Surfactant Protein C (SFTPC), and Club Cell Secretory Protein (CCSP) antibodies, the four LSC markers established previously in human LSCs [9]. Expression of MHC classes I and II was also studied. Cells were subjected to membrane fixation and permeabilization (Cytofix/

Cytoperm; BD Biosciences, San Diego, CA, <http://www.bdbiosciences.com>) prior to SFTPC and CCSP antibody incubation to account for documented intracellular expression [10, 11]. All antibodies were incubated with  $5 \times 10^5$  LSCs for 60 minutes at 4°C. The cross expression of MHC class I and II was recorded using Alexa Fluor 488- and PE-conjugated antibodies with compensation. Nonlabeled cells were used as negative controls and isotype-identical antibodies served as nonspecific binding controls. All flow cytometry was performed on a CytoFlex Flow Cytometer (Beckman Coulter, Brea, CA, <https://www.beckmancoulter.com>) and all data were analyzed with FCS Express software (De Novo Software, Glendale, CA, <https://www.denovosoftware.com>).

### Immunocytochemistry on Lung Spheroids and LSCs

LSCs were plated onto fibronectin-coated 4-chamber Millicell culture slides (EMD Millipore, Billerica, Massachusetts, <http://www.emdmillipore.com>). They were fixed with 4% paraformaldehyde (PFA) and blocked/permeabilized with Dako Protein Block Solution (Dako, Carpinteria, CA, <http://www.dako.com>) containing 0.1% saponin. Subsequently, the cells were treated with anti CD105, CD90, SFTPC, CCSP, and Aquaporin 5 antibodies overnight at 4°C followed by incubation with secondary antibodies. Lung spheroids were frozen in O.C.T. compound (Sakura Finetek, Tokyo, Japan, <http://www.sakura-finetek.com>) and cryosectioned into 5 μm sections. Sections were then incubated with antibodies against SFTPC, CCSP, CD105, CD90, Aquaporin 5, Keratin 5, CD31, and CD45. Alexa Fluor 488 and Texas Red conjugated secondary antibodies (Abcam, Cambridge, MA, <http://www.abcam.com>) were used for detection. Images were taken with an epifluorescent microscope (Olympus IX81; Olympus, Center Valley, PA, <http://www.olympusamerica.com>).

### In Vitro Endothelial Tube Formation Assay

Proangiogenic effects of rat LSCs were demonstrated through an endothelial cell tube-formation assay. Human umbilical vein endothelial cells (HUVECs, American Type Culture Collection, Manassas, VA, <http://www.atcc.org>) were seeded onto growth factor-reduced Matrigel in 96-well plates at a density of 10,000 cells per well. The cells were cultured in 100 μl of either IMDM or LSC-conditioned IMDM. Ten hours later, the wells were imaged with a Nikon TE-200 white light microscope (Nikon, Tokyo, Japan, <http://www.nikon.com>). HUVECs produced tubules that were measured in length (μm) with NIH Image J software.

### Animal Procedures

Six to eight-week-old female WKY or BN rats were randomized into 4 treatment groups. (a) WKY Control (Bleo + saline): intratracheal instillation of 1.5 U/kg body weight bleomycin (EMD Millipore, Billerica, MA, <http://www.emdmillipore.com/>) in 250 μl of PBS, followed by tail vein injection of 300 μl PBS after 24 hours; (b) BN Control (Bleo + saline): intratracheal instillation of 1.5 U/kg body weight bleomycin in 250 μl of PBS, followed by tail vein injection of 300 μl PBS after 24 hours; (c) WKY syngeneic therapy (Bleo + <sub>syn</sub>LSC): intratracheal instillation of 1.5 U/kg body weight bleomycin in 250 μl of PBS, followed by tail vein injection of  $5 \times 10^6$  WKY LSCs in 300 μl PBS after 24 hours. (d) BN allogeneic therapy (Bleo + <sub>allo</sub>LSC): intratracheal instillation of 1.5 U/kg body weight bleomycin in 250 μl of PBS, followed by tail vein injection of  $5 \times 10^6$  WKY LSCs in 300 μl PBS after 24 hours. All tracheal instillations were done using a syringe and gavage needle. A cohort of rats was injected with EGFP (Vector Biolabs, Malvern,

PA, www.vectorbiolabs.com) transfected cells to enable histological detection of transplanted cells. After 14 days, all rats were euthanized, blood was drawn, and lungs were harvested for histological and PCR analysis. Rat lungs were frozen in Tissue-Tek O.C.T. compound and cryosectioned (5  $\mu$ m thickness).

### Histology

Immunofluorescence (IF) was performed on 4% PFA-fixed lung cryosections (5–10  $\mu$ m). Samples were permeabilized and blocked with Dako Protein Block Solution containing 0.1% saponin at room temperature for one hour and then incubated with primary antibodies overnight at 4°C. The samples were then incubated with secondary antibodies for 1.5 hours at room temperature. 4',6-diamidino-2-phenylindole (DAPI) was applied for 10 minutes before mounting. All wash steps were performed with nonsterile PBS. The following antibodies were used for tissue IF: Aquaporin 5, SFTPC, von Willebrand Factor (vWF), CD3, and CD8. Cryosections were also stained with Hematoxylin and Eosin for Ashcroft scoring, Masson's trichrome for the detection of connective tissue, and Picrosirius Red for the detection of collagen. Apoptotic cells were detected with terminal deoxynucleotidyl transferase dUTP nick-end labeling (TUNEL) assay (Roche Diagnostics, Mannheim, Germany, <http://www.roche-applied-science.com>).

### Cytokine Array

To measure systemic inflammation and immune reaction, a rat cytokine antibody array assay (Ray Biotech, Inc. Norcross, GA, www.raybiotech.com) was performed for the detection of 19 rat proteins in serum. Briefly, rat serum was obtained by centrifugation of WKY and BN rat whole blood at 2,000g for 10 minutes. The serum of three rats from the syngeneic group and three rats from the allogeneic group was diluted fivefold with blocking buffer. A 1 ml sample of each serum was incubated with the cytokine array membranes overnight at 4°C. A series of washes was followed by incubation of biotinylated antibodies for 2 hours at room temperature. The membranes were then treated with HRP-Streptavidin overnight at 4°C before being exposed to chemiluminescent buffer. Chemiluminescence was detected with the Biorad Chemi-Doc MP Imaging System (Bio-Rad, CA, USA, <http://www.bio-rad.com>). Cytokine arrays were analyzed using Image Lab software. The relative expressions of individual proteins were standardized to the positive control signal.

### Cell Retention Analysis by Quantitative PCR

Quantitative PCR was performed 24 hours after cell injection in five animals from each cell-injected group to quantify cell retention/engraftment. We injected LSCs from male donor WKY rats into WKY or BN female recipients to use the detection of the *SRY* gene located on the Y chromosome as target. The whole lung was harvested, weighed, and homogenized. Genomic DNA was isolated from aliquots of the homogenate corresponding to 12.5 mg of pulmonary tissue, using commercial kits (DNA Easy minikit, Qiagen, Germantown, MD, <https://www.qiagen.com>). The TaqMan assay (Applied Biosystems, Foster City, CA, <http://www.appliedbiosystems.com>) was used to quantify the number of transplanted cells with the rat *SRY* gene as template (forward primer: 5'-GGA GAG AGG CAC AAG TTG GC-3', reverse primer: 5'-TCC CAG CTG CTT GCT GAT C-3', TaqMan probe: 6FAM CAA CAG AAT CCC AGC ATG CAG AAT TCA G TAMRA, Applied Biosystems). A standard curve was generated with multiple dilutions of genomic DNA isolated from male lungs to quantify the absolute gene copy

numbers. All samples were spiked with equal amounts of female genomic DNA as control. The copy number of the *SRY* gene at each point of the standard curve was calculated with the amount of DNA in each sample and the mass of the rat genome per cell. For each reaction, 50 ng of template DNA was used. Real time PCR was performed with an Applied Biosystems 7900 HT Fast real-time PCR System. All experiments were performed in triplicate. Cell numbers per mg of lung tissue and percentages of retained cells were calculated.

### Statistics

All results are presented as means  $\pm$  SD unless otherwise specified. Comparisons between any two groups were performed using 2-tailed unpaired Student's *t* tests with a 95% confidence interval. One-way ANOVA analysis of variance was used to compare means among more than two groups, followed by post hoc Bonferroni correction. Statistical significance was achieved at  $p < .05$ .

### Study Approval

All animal work was compliant with the Institutional Animal Care and Use Committee at North Carolina State University.

## RESULTS

### Growth Potential and Antigenic Phenotypes of LSCs

A schematic of overall tissue-to-cell processing and rat injection procedure are presented in Figure 1A. Lung tissue explants were plated on fibronectin-coated petri dishes to allow cells to outgrow (Fig. 1BI). The outgrowth cells were collected and plated into low attachment flasks for the formation of lung spheroids (or LSs) (Fig. 1BII). The LSs were collected and replated onto fibronectin-coated flasks to dissociate into LSCs (Fig. 1BIII), which are the final cell therapy products. LSCs were able to undergo 4 to 6 doublings in 3 passages (Fig. 1C).

Immunocytochemistry was used to identify the cell phenotypes in LSs. CD105<sup>+</sup> and CD90<sup>+</sup> stromal cells formed an outer shell around clustered SFTPC<sup>+</sup> (alveolar type II epithelial cells) and CCSP<sup>+</sup> (club cells) lung progenitor cells (Fig. 1DI–1DIV). Expression of epithelial markers (e.g., AQP5<sup>+</sup>, KRT5<sup>+</sup>) were evident throughout the spheres (Fig. 1DV, 1DVI). Endothelial marker CD31 and hematopoietic marker CD45 were not expressed (Fig. 1DVII, 1DVIII). As derivatives of lung spheroids, LSCs expressed CD105, CD90, SFTPC, and CCSP (Fig. 1EI–1EIV). In addition, stromal CD90<sup>+</sup> cells were costained with AQP5<sup>+</sup> and SFTPC<sup>+</sup> cells to demonstrate the heterogeneous composition of the LSCs (Fig. 1EV, 1EVI). Flow cytometry analysis confirmed the expressions of those markers (Fig. 1F) and the increased expression of progenitor markers CCSP and SFTPC in LSCs compared to explant derived cells (EDCs; Supporting Information Fig. 1) Double staining showed that rat LSCs express MHCI, an intracellular histocompatibility marker found in all nucleated cells, but very little extracellular MHCII, which is only expressed in antigen presenting cells (Fig. 1G).

### LSCs Promote Angiogenesis and Release Antifibrotic Factors

Mounting lines of evidence suggest that the therapeutic effects of stem cell treatments are owed in large part to paracrine mechanisms rather than direct regeneration [12–16]. The promising stem cell injections in rats in our lab prompted us to explore

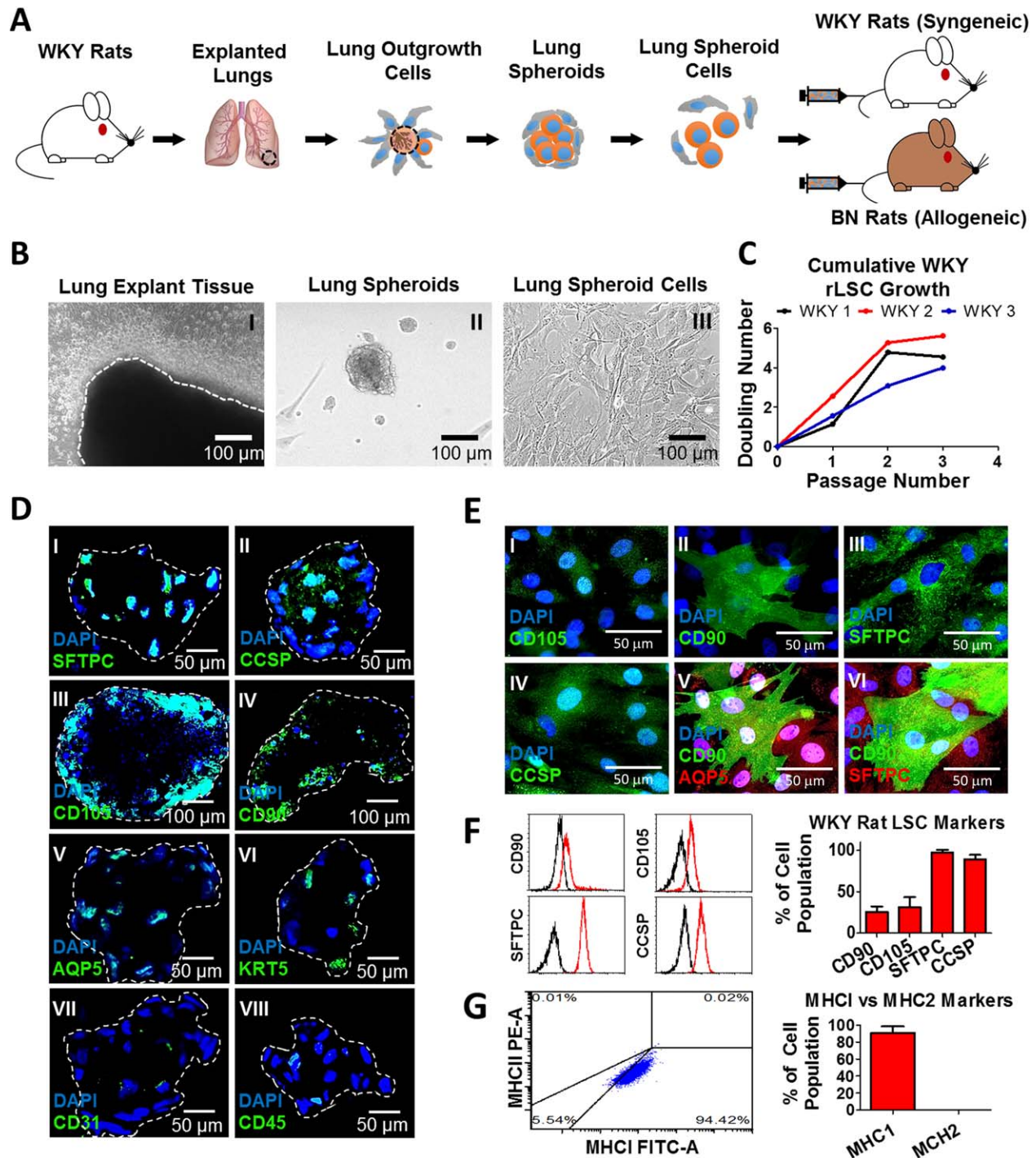


**Figure 1.** Generation of lung spheroids and LSCs. **(A):** A schematic showing the design of overall cell processing and animal injections. Lung outgrowth cells are harvested from the distal region of excised lungs from WKY rats. The cells are allowed to self-aggregate in an ultra-low attachment flask where they form spheroids before being plated back onto a fibronectin coated flask where they disassociate into the final injectable product: rat LSCs. **(B):** Lung explant cells are shown migrating away from the bulk tissue **(BI)**, agglomerating into spheroids **(BII)**, and being re-plated as LSCs **(BIII)**. **(C):** A cumulative growth curve of population doubling over time showing the growth potential of rat LSCs. **(D, E):** Representative fluorescent micrographs showing the expressions of various cellular markers in lung spheroids and LSCs. **(F):** Flow cytometry histogram and bar graph showing the relative expressions of CD90, CD105, SFTPC, and CCSP in rat LSCs. **(G):** Flow cytometry dot plot and bar graph showing the relative expressions of MHC I and MHC II in rat LSCs. Abbreviations: BN, Brown Norway; CCSP, club cell secretory protein; DAPI, 4',6-diamidino-2-phenylindole; LSCs, lung spheroid cells; MHC, major histocompatibility complex; SFTPC, surfactant protein C; WKY, Wistar-Kyoto.

proteins released by LSCs. As part of a related study, mass spectroscopy was run on the LSC conditioned media, revealing a myriad of pro-angiogenic and antifibrotic proteins (Supporting

Information Fig. 2), possible agents for therapy that will be further evaluated in subsequent studies. Human umbilical vein endothelial cells (HUVECs) were cultured in LSC-conditioned media (Fig.

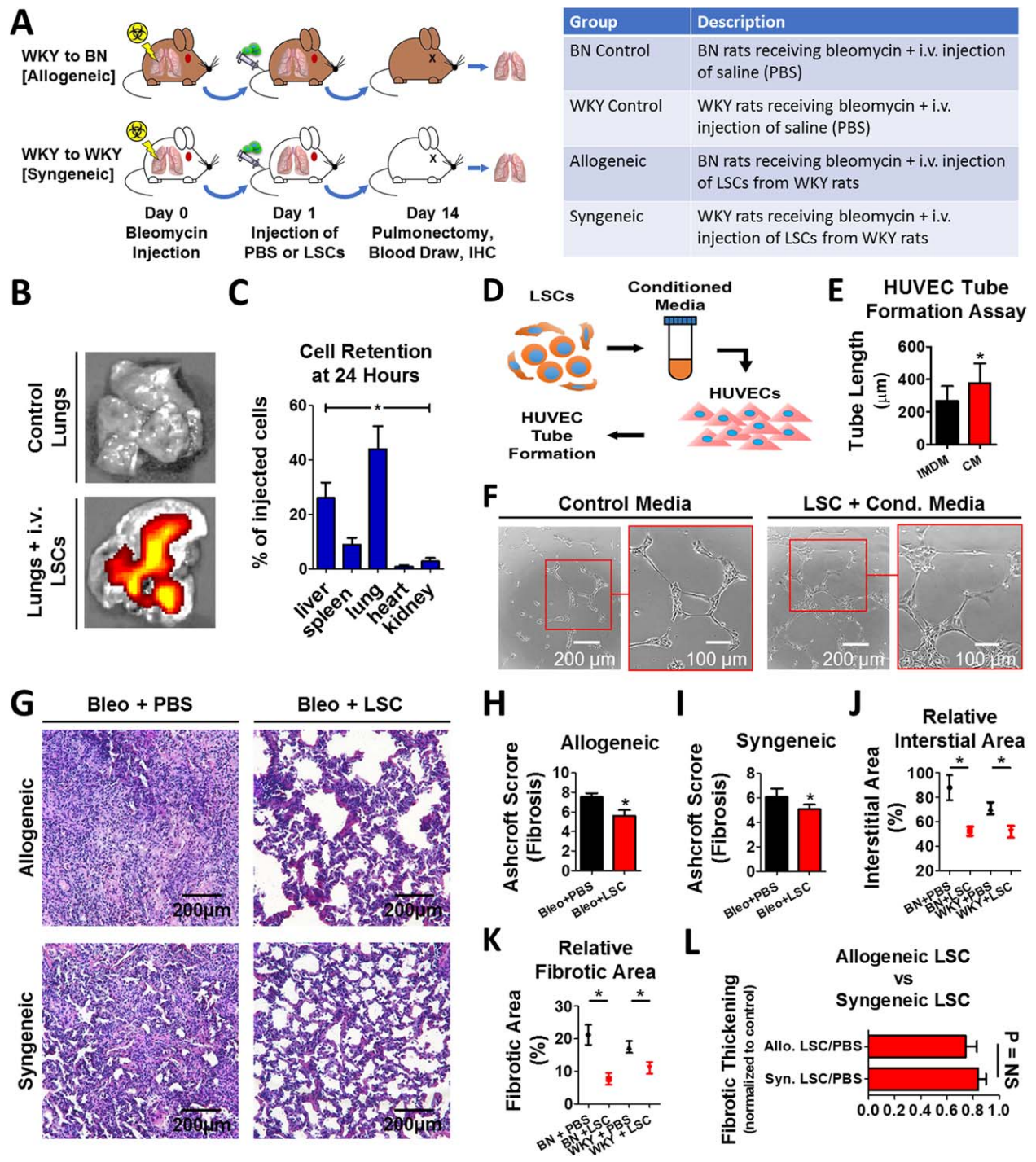


**Figure 2.** Benefits of intravenous delivery of allogenic LSCs and in vitro LSC-conditioned media assay. **(A):** Illustrated summary of animal study design and experimental groups. **(B):** Representative fluorescent imaging of excised lungs showing the effective delivery of LSCs (red) via intravenous tail vein injection. **(C):** Bar graph showing the relative engraftment of rat LSCs in main organs post intravenous injection. **(D):** A schematic illustrating the culture of HUVECS in LSC-conditioned media. **(E):** Bar graph summarizing the effects of LSC conditioned media on HUVEC tube length. **(F):** Representative white-light micrographs showing the HUVEC tube formations in plain IMDM and rat LSC conditioned media. **(G):** Representative H&E stained micrographs of excised rat lungs 14 days after LSC or saline treatments. **(H, I):** Bar graphs summarizing the Ashcroft (fibrotic thickening) scores after saline or LSC treatment. **(J):** Bar graph summarizing the relative interstitial area from H&E histology for the saline and LSC treatments. **(K):** Bar graph summarizing the relative fibrotic area from Picrosirius Red histology for the saline and LSC treatments. **(L):** Bar graph comparing the treatment efficacies from allogeneic and syngeneic LSCs as normalized to the corresponding control groups. \* indicates  $p < .05$  when compared to the control group. Abbreviations: BN, Brown Norway; HUVEC, human umbilical vein endothelial cells; IMDM, Iscove's modified Dulbecco's medium; LSCs, lung spheroid cells; PBS, phosphate-buffered saline; WKY, Wistar-Kyoto.

2D) to evaluate the *in vitro* effects of the pro-angiogenic factors. The average tube lengths of HUVECs cultured in LSC conditioned media were greater than those cultured in IMDM ( $375.7 \pm 9.9 \mu\text{m}$  vs.  $268.4 \pm 7.2 \mu\text{m}$ ; Fig. 2E, 2F). Taken together, the data suggest that LSCs have the potential to reduce fibrosis through paracrine mechanisms while promoting angiogenesis.

### Intravenous Delivery of Allogeneic LSCs Attenuates Fibrotic Progression

The animal study design is illustrated and summarized in Figure 2A. To create the pulmonary fibrosis model, bleomycin was given to WKY (syngeneic group) or BN (allogeneic group) rats intratracheally on Day 0. On Day 1, the rats were injected intravenously (via the tail vein) with LSCs derived from WKY rats. Control animals received intravenous injection of saline. On Day 14, all animals were sacrificed for histology. Fluorescent imaging revealed that intravenous injection successfully delivered LSCs (DiI-labeled) into the lungs (Fig. 2B). Quantitative PCR was used to determine the cell retention dynamics in the liver, spleen, lung, heart, and kidneys. Roughly 44% of all cells injected remained in the lungs 24 hours post injection (Fig. 2C). Another 26% of cells were lost in the liver and 9% in the spleen. H&E staining revealed severe fibrotic thickening in the saline-injected group (Fig. 2G). Ashcroft scoring (indicating the degree of fibrotic thickening) confirmed that, compared to the saline control, both allogeneic ( $7.5 \pm 0.2$  vs.  $5.6 \pm 0.3$ ) and syngeneic ( $6.1 \pm 0.3$  vs.  $5.1 \pm 0.2$ ) LSCs reduced fibrotic thickening (Fig. 2H, 2I). The H&E histology was quantified for relative interstitial tissue area using Image J software (Fig. 2J). A more advanced progression of fibrosis was seen in the controls for both allogeneic ( $88.01\% \pm 10.18\%$  vs  $52.46\% \pm 3.806\%$ ) and syngeneic ( $71.10\% \pm 4.814\%$  vs  $51.96\% \pm 4.919\%$ ) treatment. In addition, picrosirius red histology was quantified for collagen deposition. The relative fibrotic areas were counted (allogeneic ( $21.20\% \pm 3.044\%$  vs  $7.695\% \pm 1.838\%$ ); syngeneic ( $17.47\% \pm 1.792\%$  vs  $11.08\% \pm 1.827\%$ )) and follow a comparable pattern to the interstitial area counts (Fig. 2K), reflecting a possible correlation between the interstitial thickening and increased collagen deposition. A head-to-head comparison between allogeneic and syngeneic LSC treatment showed no significant difference in fibrotic thickening when normalized to the corresponding PBS control group (Fig. 2L). This data suggests that allogeneic LSCs are equally effective as syngeneic LSCs in mitigating the onset of fibrosis in rats.

### LSC Treatment Attenuates Connective Tissue and Collagen Buildup in Post-Injury Lungs

The overall connective tissue deposition in the lungs treated with LSCs is evidently less than that of the lungs injected with just PBS as shown in the low power Masson's trichrome staining in Figure 3A. The same result is demonstrated at higher magnifications, with more emphasis on the blue-stained regions of connective tissue (Fig. 3C). Similarly, the lungs injected with LSCs show less pervasive deposition of collagen (deep red/pink), as exemplified by the Picrosirius Red staining in Figure 3B and three-dimensional (3D) at low and high magnifications, respectively. Picrosirius staining was additionally quantified in Figure 2K to assess relative fibrotic areas.

### Allogeneic LSC Therapy Protects Endogenous Pneumocytes in Post-Injury Lungs

The expression of aquaporin-5 membrane protein (labeling alveolar Type I pneumocytes) was significantly higher in the allogeneic LSC-treated groups ( $0.18 \pm 0.054$  vs.  $0.02 \pm 0.004$  pixels/total pixels) and syngeneic LSC-treated groups ( $0.55 \pm 0.032$  vs.  $0.15 \pm 0.030$  pixels/total pixels) as compared to the corresponding control groups (Fig. 4A–4C). Such protective effects were more profound in regions around the engrafted LSC foci (red, Fig. 4A). Similar protection was also seen for SFTPC<sup>+</sup> alveolar Type II pneumocytes. The allogeneic ( $7.1 \pm 0.60$  vs.  $3.84 \pm 0.45$ ) and syngeneic ( $14.02 \pm 1.63$  vs.  $8.27 \pm 0.65$ ) LSC treatments resulted in higher SFTPC counts compared to the saline control (Fig. 4E–4G). When normalized to their saline controls, there was no significant difference between allogeneic and syngeneic LSC treatments (Fig. 4D, 4H). This suggests allogeneic LSCs are equally effective as syngeneic LSCs in protecting pneumocytes after the bleomycin-induced injury in rats.

### Allogeneic LSC Therapy Inhibits Apoptosis and Promotes Angiogenesis in Post-Injury Lungs

TUNEL assay analysis of excised rat lungs revealed that cell apoptosis was significantly higher in the saline-treated control groups (Fig. 5A). Compared to controls, TUNEL expression is significantly lower with the allogeneic ( $9.96\% \pm 2.02\%$  vs.  $2.17\% \pm 0.42\%$ ) and syngeneic ( $1.40\% \pm 0.18\%$  vs.  $0.83\% \pm 0.16\%$ ) LSC treatments (Figs. 5C, 5D). Pulmonary vWF (Fig. 5B) expression (endothelial marker) was much denser after allogeneic ( $0.032 \pm 0.007$  vs.  $0.062 \pm 0.011$ ) and syngeneic ( $0.039 \pm 0.003$  vs.  $0.090 \pm 0.016$ ) LSC treatment (Fig. 5E, 5F). When normalized to the saline control, there is no significant difference in TUNEL or vWF expression between allogeneic and syngeneic LSC treatment (Fig. 5G, 5H), suggesting allogeneic LSCs are equally effective as syngeneic LSCs in inhibiting pulmonary apoptosis and promoting angiogenesis.

### Allogeneic LSC Therapy Elicits No Significant Systemic or Local Immune-Rejection

On Day 14, cytokine array analysis on 19 well-known inflammatory, immune response, wound healing, and epithelium proliferation cytokines revealed there were no significant differences between serum samples from allogeneic LSC- and syngeneic LSC-treated animals (Fig. 6A, 6B), suggesting that no systemic rejection had occurred. The numbers of CD3- and CD8-positive T cells in the lungs (Fig. 6C) were assessed to determine local immune rejection. The data showed no significant difference between the allogeneic LSC and syngeneic LSC groups for either CD3 ( $4.86 \pm 0.36$  allo. vs.  $5.20 \pm 0.42$  syn., Fig. 6D) or CD8 ( $0.21 \pm 0.05$  allo. vs.  $0.27 \pm 0.05$  syn., Fig. 6E) expression. These datasets suggest allogeneic LSC transplantation did not elicit systemic or local immune rejection.

## DISCUSSION

The transplantation of autologous stem cells in animal models has been validated extensively in literature in a wide berth of pathologies [3, 5, 17]. Consequently, the success rate of the autologous paradigm, driven by its low propensity for graft-vs.-host disease, has facilitated its transition into clinical treatments. However, autologous cell therapy products are expensive and time consuming to make. In addition, patient age and disease progression can

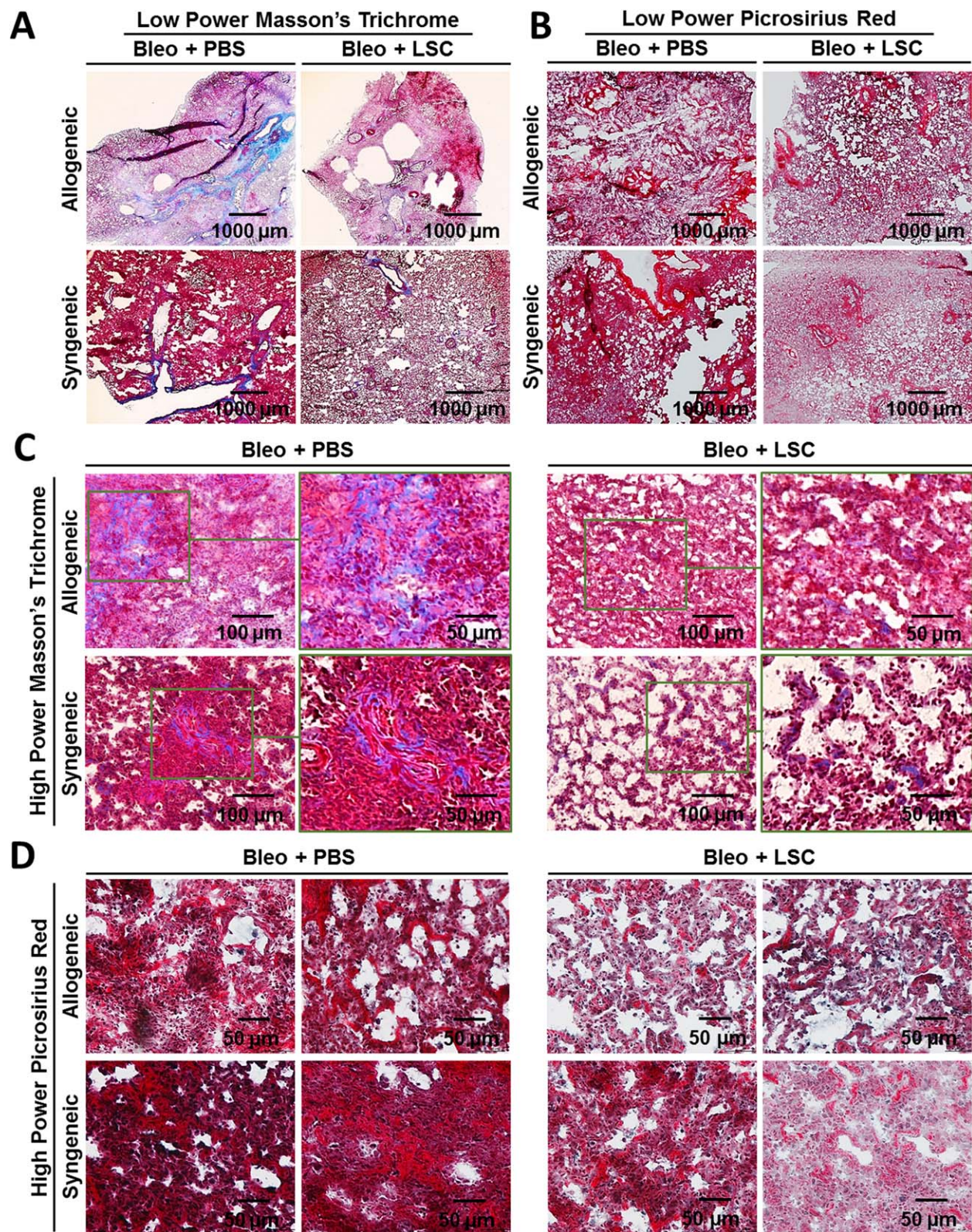


**Figure 3.** LSC treatment attenuates connective tissue and collagen buildup. **(A):** Low power micrographs showing connective tissue build-up in Masson's trichrome stained lung sections. **(B):** Low power micrographs showing collagen deposition in Picrosirius Red stained lung sections. **(C, D):** High power micrographs of lung sections stained with Masson's Trichrome for connective tissue and Picrosirius Red for collagen, respectively. Abbreviations: LSCs, lung spheroid cells; PBS, phosphate-buffered saline.

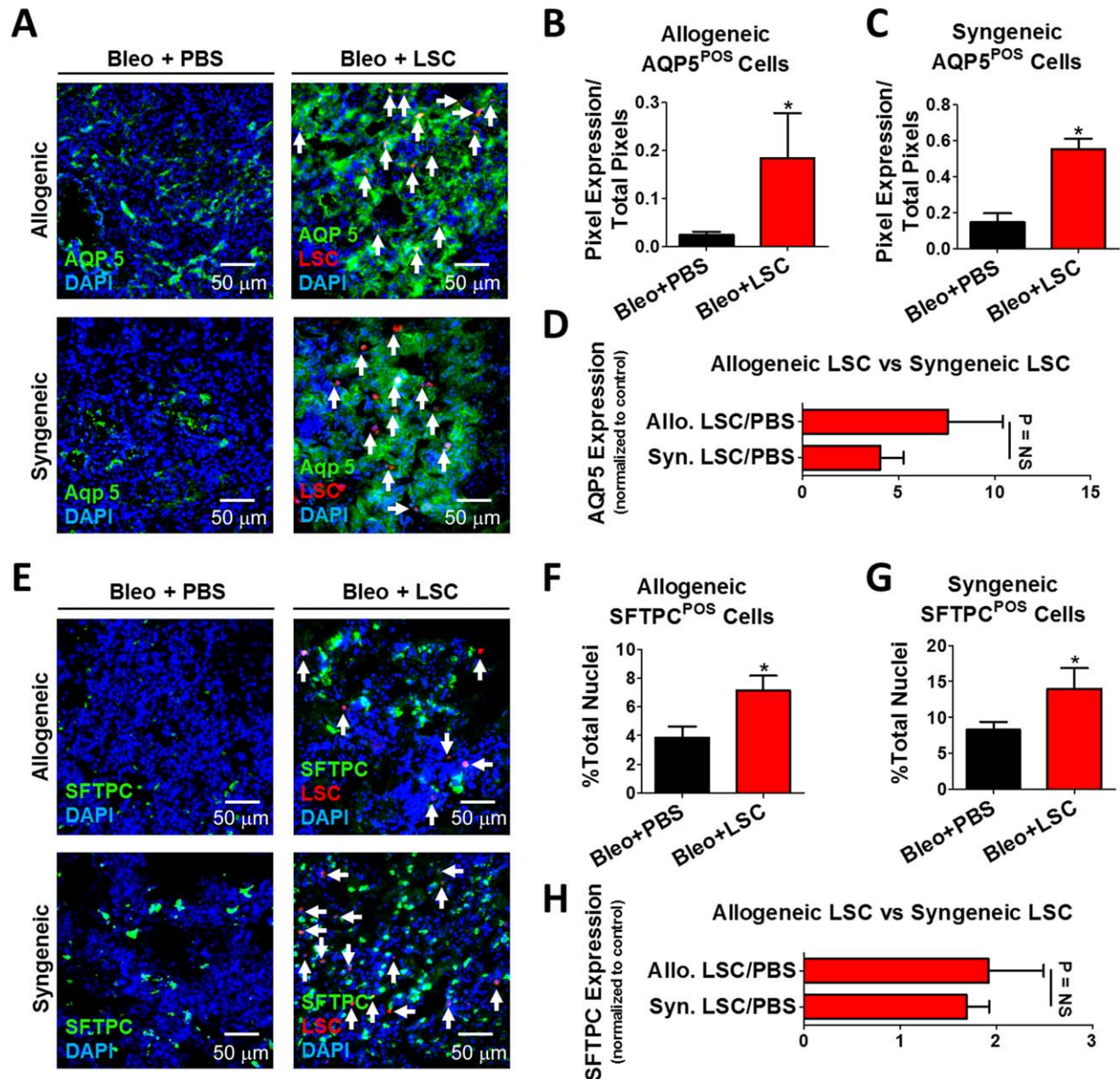


**Figure 4.** Allogeneic LSC treatment protects endogenous pneumocytes. **(A):** Representative micrographs showing Aquaporin 5-positive pneumocytes (green) and LSC engraftment (red with white arrows). **(B, C):** Bar graphs showing the effects of allogeneic and syngeneic LSC treatment on Aquaporin 5-positive pneumocytes compared with each control group. **(E):** Representative micrographs showing SFTPC positive pneumocytes (green) and LSC engraftment (red with white arrows). **(F, G):** Bar graphs summarizing the count of SFTPC positive pneumocytes (green) and LSC engraftment (red with white arrows). **(D, H):** Bar graph showing the control-normalized expression of Aquaporin-5 and SFTPC, respectively, after rat allogeneic and syngeneic LSC treatment. \* indicates  $p < .05$  when compared with the control group. Abbreviations: DAPI, 4',6-diamidino-2-phenylindole; LSCs, lung spheroid cells; PBS, phosphate-buffered saline; SFTPC, surfactant protein C.

result in variations in cell potency [18]. In this study, we demonstrated the safety and efficacy of an intrinsic lung-derived cell therapy product in a bleomycin-induced rat model of pulmonary fibrosis. Allogeneic cell therapy for lung diseases has been pursued in previous research endeavors and current phase I clinical trials, but almost exclusively with MSCs [5, 19–21]. In contrast, the use of intrinsic distal lung-derived cells represents a new approach [20]. LSCs benefit from a self-agglomerating 3D sphere culture system which has been shown to recapitulate the *in vivo* environment and enhance the innate stemness of cells [22]. The cultured spheres have been shown to self-organize in niche-like layers that bring out their stem cell qualities (Supporting Information Fig. 1)

through cell-cell interactions, which are built upon by the heterogeneity of the cell populations in the spheres [23]. The prominent markers expressed in LSCs are CD105, CD90, SFTPC, and CCSP, indicating a stromal-epithelial mixture in which progenitor type II alveolar epithelial cells, together with club cells, can build on the well-documented benefits of mesenchymal cells native to the lung parenchyma [24]. Based on the expression of progenitor markers as well as the general lack of MHCII expression, LSCs can elicit abundant regenerative potential but overall immune quiescence [25, 26]. Once intravenously injected, most of the cells end up in the lungs, as demonstrated by the quantitative PCR analysis in Figure 2C. Previous researchers have documented the efficacy

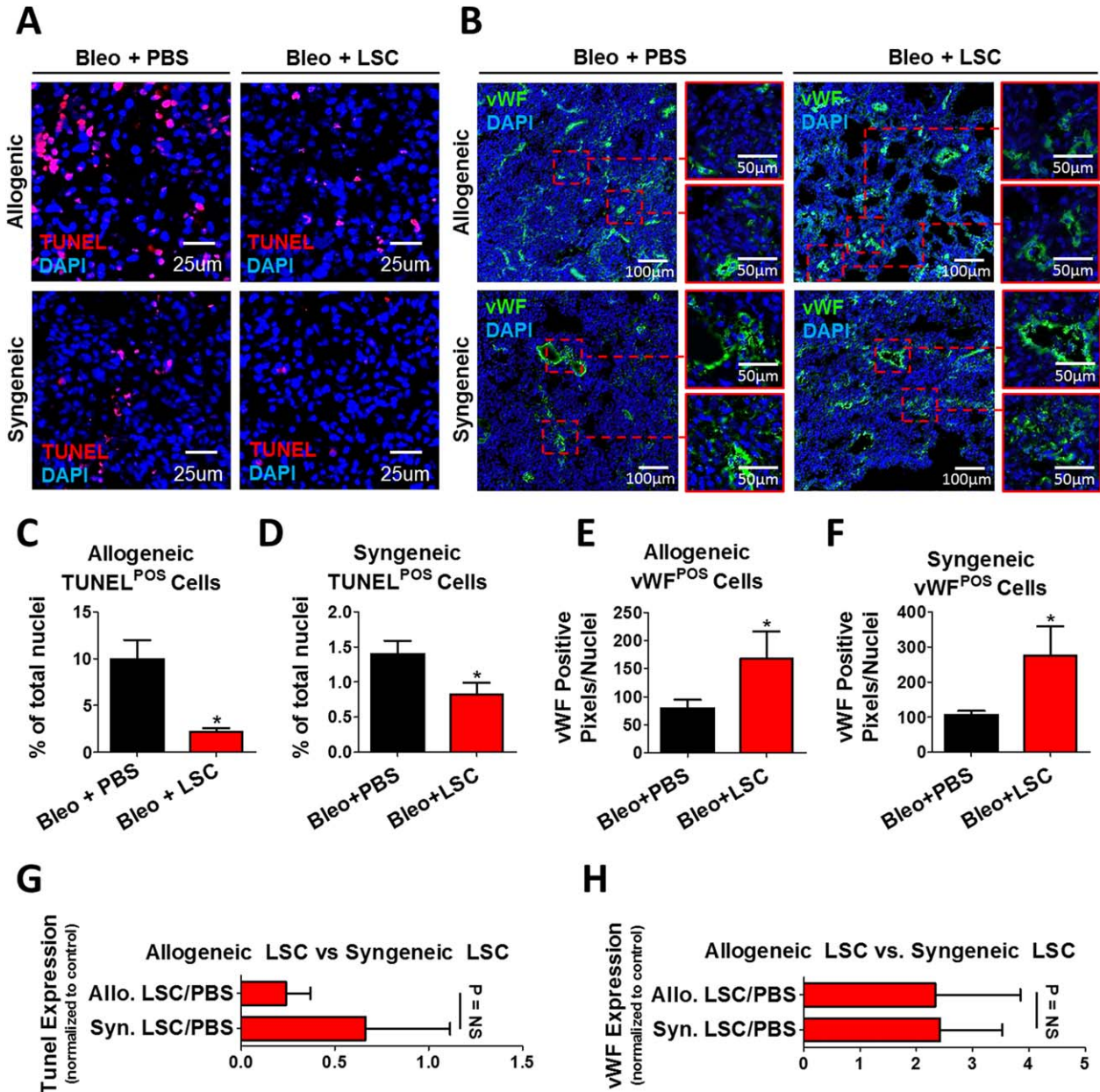


**Figure 5.** Allogeneic LSC treatment inhibits apoptosis but promotes angiogenesis in bleomycin-induced fibrotic lungs. **(A):** Representative fluorescent micrographs showing TUNEL-positive apoptotic cells (red). **(B):** Representative fluorescent micrographs showing vWF-positive endothelial cells (green). **(C, D):** Bar graphs summarizing the TUNEL-positive cells for the saline control and LSC groups in both allogeneic and syngeneic experiments. **(E, F):** Bar graphs summarizing the vWF expression for the saline control and LSC groups in both allogeneic and syngeneic experiments. **(G, H):** Bar graph showing the control-normalized expression of TUNEL and vWF, respectively, after rat allogeneic and syngeneic LSC treatment. \* indicates  $p < .05$  when compared to the control group. Abbreviations: DAPI, 4',6-diamidino-2-phenylindole; LSCs, lung spheroid cells; PBS, phosphate-buffered saline; vWF, von Willebrand Factor.

of the i.v. route for stem cell delivery to the lung as a result of the pulmonary first-pass effect [27, 28]. In the future, to avoid the introduction of undefined proteins into human patients and prevent antibiotic resistant pathogens, it will be necessary to culture the cells in low to no FBS media with little to no antibiotics. This is especially true for the EDC and LSC stages, where 20% FBS is used.

A large body of pathological studies indicate that IPF is characterized by continuous debilitation of the alveolar epithelium, which is then accompanied by abnormal fibroblast activation and collagen deposition [26, 29] In this study, the health of the alveolar epithelium is evaluated, in part, by the quantification of endogenous

Type I and II epithelial cells, which can be traced by the Aquaporin 5 and SFTPC markers, respectively (Fig. 4A–4H). The higher densities of Type I and II pneumocytes in the allogeneic and syngeneic LSC-treated lungs reflect the benefits of LSC therapy over the saline controls in protecting pneumocytes after the bleomycin-induced lung injury. This result is supported by H&E staining showing lower relative interstitial areas (Fig. 2J), more porosity (i.e., greater surface area for gas exchange,) and less fibrotic thickening in the LSC-treated groups (Fig. 2G–2I). In addition, the lungs treated with LSC's show less connective tissue and collagen deposition (Fig. 4A–4D), as well as less relative fibrotic areas (Fig. 2K).

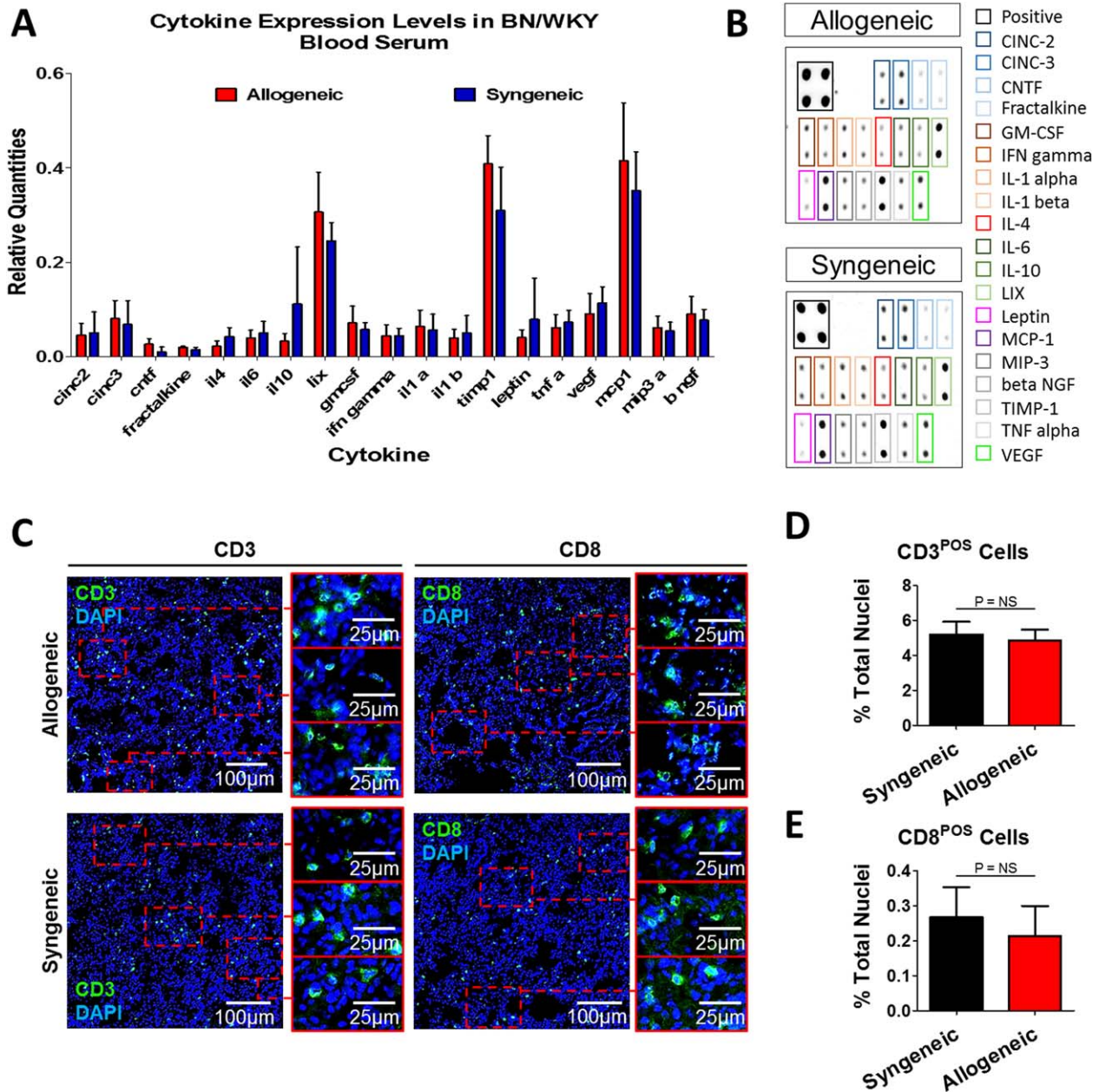


**Figure 6.** Systemic and local immunogenicity by allogeneic LSC treatment. **(A, B):** Quantitation and representative protein arrays showing immune response and inflammatory cytokines in the sera of rats treated with allogeneic or syngeneic LSCs. **(C):** Representative fluorescent micrographs showing CD3- and CD8-positive T cells in the lungs treated with allogeneic or syngeneic LSCs. **(D, E):** Bar graphs summarizing the CD3 and CD8 expression (counts), respectively, in allogeneic and syngeneic treatment. Abbreviations: BN, Brown Norway; WKY, Wistar-Kyoto; DAPI, 4',6-diamidino-2-phenylindole.

It is not just the epithelium, however, that suffers in fibrotic lungs [30]. In the bleomycin model, damage to the venous and arterial endothelium manifests in the accumulation of interstitial edema which eventually leads to capillary attenuation and cell swelling, a common precursor to apoptosis [31–33]. If follows then, that in searching for therapeutic options to combat the progression or achieve the reversal of pulmonary fibrosis, it is necessary to reestablish the health of damaged endothelium [34–36]. One way of assessing endothelial health is to look for the formation of new blood vessels (angiogenesis) as part of the healing process in damaged tissue post treatment [37]. The measurements of pulmonary vessel densities with external diameters less than 100

µm demonstrate the therapeutic potential of allogeneic LSCs in protecting original and/or generating new endothelium in fibrotic lungs (Fig. 5B, 5E, 5F, 5H; Supporting Information Fig. 3). The HUVEC tube formation assay (Fig. 2D–2F) performed using cell media conditioned with rat LSCs further confirms the pro-angiogenic nature of LSCs. Our previous studies suggest that secreted factors from adult stem cells play an important role in stem cell-mediated tissue repair [38, 39].

To rule out systemic immunogenicity from allogeneic LSC treatment, we performed a cytokine array assay on blood serum samples from syngeneic and allogeneic LSC-treated rats. The comparison revealed no significant difference in the levels of immune response

(cinc2, cinc3, GM-CSF, IFN gamma, IL-4, IL-6, LIX, TNF-Alpha) and inflammatory response cytokines (cinc2, cinc3, Fractalkine, IL-1 a, IL-1 b, IL-4, IL-6, LIX, MCP1, MIP-3, TNF-Alpha) (Fig. 6A, 6B). Proteins involved in wound healing (Fractalkine, TIMP-1, and VEGF) and epithelial cell proliferation (GM-CSF and IL-6) also showed similar expression levels between allogeneic and syngeneic groups (Fig. 6A, 6B). To assess local immune response, we quantified CD3- and CD8-positive T cells in the lung and found there were no significant differences between allogeneic and syngeneic LSC treatment (Fig. 6C–6E). The collective data on T lymphocyte expression in lung tissue and the cytokine levels in serum samples confirm there is no significant immunological/inflammatory response resulting from allogeneic LSC treatment. It is possible that the histocompatibility characteristics of the LSCs (discussed above) are playing a role in the apparent immune quiescence. The lack of MHCII antigens inhibits T-Helper Cell recognition of LSCs while the presence of MHCI antigen provides protection from natural killer Cell-mediated responses [40]. Moreover, the mesenchymal subpopulation in LSCs may be immuno-evasive [41]. The lack of immune reactivity facilitates and favors the translation of this allogeneic cell therapy in human patients who would otherwise require immunosuppressant medication to accept the cells. This preclinical study in rats paves the way for investigational new drug (IND)-enabled human studies using autologous or allogeneic LSCs for the treatment of IPF. Future studies will focus on the elucidation of mechanisms underlying the therapeutic benefits of allogeneic LSCs and should also explore the application of LSCs for other lung diseases such as COPD and fibrocavernous pulmonary tuberculosis.

## CONCLUSION

We have demonstrated the safety and efficacy of allogeneic LSC treatment in attenuating the progression and severity of fibrosis,

decreasing apoptosis, protecting alveolar structures, and increasing angiogenesis in a rat model of pulmonary fibrosis. The use of allogeneic stem cell treatments has the potential to change the way we perform cell therapies. It would allow for the growth of large quantities of cells from a number of sources, including donated lungs not used for transplantations, surgical discards, and lungs from recently deceased cadavers [40]. These cells could be expanded in a centralized, quality-controlled facility and stored for future use, potentially making the therapeutic process much faster and more cost-effective. Our results warrant further research in large animal models of pulmonary fibrosis and as part of IND-enabled human studies before transitioning into the clinical arena.

## ACKNOWLEDGMENTS

This study was supported by the U.S. National Institute of Health (HL123920, HL137093), a UNC General Assembly Research Opportunities Initiative award, a NC State Chancellor's Innovation Fund, a NC State Comparative Medicine Institute Seed Grant, and National Natural Science Foundation of China 81370216.

## AUTHOR CONTRIBUTIONS

J.C., P-U.D., M.T.H., K.K., M.R., D.P., and K.C.: conception, design, analysis, and interpretation of data; J.C., and K.C.: manuscript writing; K.C.: final approval of manuscript; J.C., M.T.H., K.K., M.R., J.T., P-U.D., A.V., T.A., Y.L., J.L., B.N., Y.C., T.C., L.J.L., D.P., and K.C.: accountability for all aspects of the work.

## DISCLOSURE OF POTENTIAL CONFLICTS OF INTEREST

The authors indicated no potential conflicts of interest.

## REFERENCES

- Raghu G, Weycker D, Edelsberg J et al. Incidence and prevalence of idiopathic pulmonary fibrosis. *Am J Respir Crit Care Med* 2006; 174:810–816.
- Ratner M. Landmark approvals in idiopathic pulmonary fibrosis. *Nat Biotechnol* 2014;32:1069–1070.
- Baker AH, Sica V, Work LM et al. Brain protection using autologous bone marrow cell, metalloproteinase inhibitors, and metabolic treatment in cerebral ischemia. *Proc Natl Acad Sci USA* 2007;104:3597–3602.
- Hong KU, Reynolds SD, Watkins S et al. Basal cells are a multipotent progenitor capable of renewing the bronchial epithelium. *Am J Pathol* 2004;164:577–588.
- Lee JW, Fang X, Gupta N et al. Allogeneic human mesenchymal stem cells for treatment of E. coli endotoxin-induced acute lung injury in the ex vivo perfused human lung. *Proc Natl Acad Sci USA* 2009;106:16357–16362.
- Tremp M, Meyer Z, Schwabedissen M, Kappos EA et al. The Regeneration potential after human and autologous stem cell transplantation in a rat sciatic nerve injury model can be monitored by MRI. *Cell Transplant* 2015;24:203–211.
- Gorin NC. Autologous stem cell transplantation in acute myelocytic leukemia. *J Am Soc Hematol* 1998;76:655–663.
- Tang YL, Zhao Q, Zhang YC et al. Autologous mesenchymal stem cell transplantation induce VEGF and neovascularization in ischemic myocardium. *Regul Pept* 2004;117:3–10.
- Henry E, Cores J, Hensley MT et al. Adult lung spheroid cells contain progenitor cells and mediate regeneration in rodents with bleomycin-induced pulmonary fibrosis. *STEM CELLS TRANSL MED* 2015;4:1–10.
- Thurm T, Kaltenborn E, Kern S et al. SFTPC mutations cause SP-C degradation and aggregate formation without increasing ER stress. *Eur J Clin Invest* 2013;43:791–800.
- Teisanu RM, Lagasse E, Whitesides JF et al. Prospective isolation of bronchiolar stem cells based upon immunophenotypic and autofluorescence characteristics. *STEM CELLS* 2009;27:612–622.
- Baraniak PR, McDevitt TC. Paracrine actions in stem cells and tissue regeneration. *Regen Med* 2010;5:121–143.
- Gnechchi M, Zhang Z, Ni A et al. Paracrine mechanisms in adult stem cell signaling and therapy. *Circ Res* 2008;103:1204–1219.
- Linero I, Chaparro O. Paracrine effect of mesenchymal stem cells derived from human adipose tissue in bone regeneration. *PLoS One* 2014;9:1–12.
- Yao LT, Zhao Q, Qin X et al. Paracrine action enhances the effects of autologous mesenchymal stem cell transplantation on vascular regeneration in rat model of myocardial infarction. *Ann Thorac Surg* 2005;80:229–237.
- Zhou S. Paracrine effects of haematopoietic cells on human mesenchymal stem cells. *Sci Rep* 2015;5:10573.
- Aki SZ, Sucak GT, Özkurt ZN et al. Allogeneic stem cell transplantation for severe aplastic anemia: Graft rejection remains a problem. *Transfus Apher Sci* 2009;40:5–11.
- Dimmeler S, Leri A. Aging and disease as modifiers of efficacy of cell therapy. *Circ Res* 2008;102:1319–1330.
- Kavanagh H, Mahon BP. Allogeneic mesenchymal stem cells prevent allergic airway inflammation by inducing murine regulatory T cells. *Allergy* 2011;66:523–531.
- Wang Z, Zhang X, Kang Y et al. Stem cell therapy for idiopathic pulmonary fibrosis: How far are we from the bench to the bedside? *J Biomed Sci Eng* 2013;6:24–31.
- Clinica Universidad de Navarra, Universidad de Navarra. Study of autologous mesenchymal stem cells to treat idiopathic pulmonary fibrosis (CMM/FPI). In: Clinical-Trials.gov. Bethesda, MD: National Library of

Medicine (US). 2000. Available at: <https://clinicaltrials.gov/show/NCT01919827> NLM Identifier: NCT01919827. Accessed June 13, 2016.

**22** Cesarz Z, Tamama K. Spheroid culture of mesenchymal stem cells. *Stem Cells Int* 2016;2016.

**23** Davis DR, Zhang Y, Smith RR et al. Validation of the cardiosphere method to culture cardiac progenitor cells from myocardial tissue. *PLoS One* 2009;4:e7195.

**24** Toonkel RL, Hare JM, Matthay MA et al. Mesenchymal stem cells and idiopathic pulmonary fibrosis potential for clinical testing. *Am J Respir Crit Care Med* 2013;188:133–140.

**25** LeGuern C, Akiyama Y, Germana S et al. Intracellular MHC class II controls regulatory tolerance to allogeneic transplants. *J Immunol* 2010;184:2394–2400.

**26** Bagnato G, Harari S. Cellular interactions in the pathogenesis of interstitial lung diseases. *Eur Respir Rev* 2015;24:102–114.

**27** Harting MT, Jimenez F, Xue H et al. Intravenous mesenchymal stem cell therapy for traumatic brain injury. *J Neurosurg* 2009;110:1189–1197.

**28** Fischer UM, Harting MT, Jimenez F et al. Pulmonary passage is a major obstacle

for intravenous stem cell delivery: The pulmonary first-pass effect. *Stem Cells Dev* 2009;18:683–692.

**29** Adamson IY, Young L, Bowden DH. Relationship of alveolar epithelial injury and repair to the induction of pulmonary fibrosis. *Am J Pathol* 1988;130:377–383.

**30** Fernando MJ, Safrin S, Weycker D et al. The clinical course of patients with idiopathic pulmonary fibrosis. *Ann Intern Med* 2005;142:963–967.

**31** Adamson IY, Bowden DH. The pathogenesis of bleomycin-induced pulmonary fibrosis in mice. *Am J Pathol* 1974;77:185–197.

**32** Moeller A, Ask K, Warburton D et al. The bleomycin animal model: a useful tool to investigate treatment options for idiopathic pulmonary fibrosis? *Int J Biochem Cell Biol* 2008;40:362–382.

**33** Chaudhary NI, Schnapp A, Park JE. Pharmacologic differentiation of inflammation and fibrosis in the rat bleomycin model. *Am J Respir Critical Care Med* 2006;173:769–776.

**34** Magro CM, Waldman WJ, Knight DA et al. Idiopathic pulmonary fibrosis related to endothelial injury and antiendothelial cell antibodies. *Human Immunol* 2006;67:284–297.

**35** Malli F, Koutsokera A, Paraskeva E et al. Endothelial progenitor cells in the pathogenesis of idiopathic pulmonary fibrosis: An evolving concept. *PLoS One* 2013;8:1–8.

**36** Adamson IYR, Bowden DH. Endothelial injury and repair in radiation-induced pulmonary fibrosis. *Lung Inj Repair* 1983;112:224–230.

**37** Gauldie J, Jordana M, Cox G. Cytokines and pulmonary fibrosis. *Thorax* 1993;48:931–935

**38** Tang J, Shen, D, Caranasos TG et al. Therapeutic microparticles functionalized with biomimetic cardiac stem cell membranes and secretome. *Nat Commun* 2017;8:13724.

**39** Luo L, Tang J, Nishi K et al. Fabrication of synthetic mesenchymal stem cells for the treatment of acute myocardial infarction in mice. *Circ Res* 2017;120:1768–1775

**40** Malliaras K, Li TS, Luthringer D et al. Safety and efficacy of allogeneic cell therapy in infarcted rats transplanted with mismatched cardiosphere-derived cells. *Circulation* 2012;125:100–112.

**41** Ankrum JA, Ong JF, Karp JM. Mesenchymal stem cells: immune evasive, not immune privileged. *Nat Biotechnol* 2014;32:252–260.



See [www.StemCells.com](http://www.StemCells.com) for supporting information available online.